

Mechanistic Studies of the Reaction of Dioxygen with Dinuclear Iron(II) Compounds to Form (μ -Peroxo)diiron(III) Complexes

Andrew L. Feig and Stephen J. Lippard*

Department of Chemistry
Massachusetts Institute of Technology
Cambridge, Massachusetts 02139

Received January 24, 1994

Carboxylate-bridged non-heme diiron(II) centers occur in several metalloenzymes involved in the biological utilization of dioxygen.^{1–5} X-ray structural information is now available for three proteins in this class, hemerythrin (Hr),⁶ the R2 protein of *Escherichia coli* ribonucleotide reductase (RR),⁷ and the hydroxylase protein of soluble methane monooxygenase (MMO).⁸ In each of the three biological systems, O₂ binds to the reduced diiron(II) core. The resultant diiron(III) peroxide species is stabilized in Hr through hydrogen bonding, whereas, in the other proteins, it reacts further through a series of not yet fully characterized steps.^{9–11} In order to understand the chemical reactivity and structural nature of species corresponding to spectroscopically identified intermediates in the reaction of the reduced proteins with O₂, we have initiated a program to investigate the corresponding reactions of known diiron(II) model complexes with dioxygen. Here we present kinetic studies of the reaction of dioxygen with three well-characterized and analogous alkoxo-bridged diiron(II) compounds (Figure 1). An analysis of the rate laws and activation parameters reveals how ligand steric factors modify the reaction pathway to the (μ -peroxo)diiron(III) species and strongly implies the need for inner sphere electron transfer chemistry.

All three diiron(II) complexes studied, [Fe₂(HPTMP)(OBz)]-(BPh₄)₂ (**1a**),^{12,13} [Fe₂(HPTP)(OBz)](BPh₄)₂ (**2a**),¹⁴ and [Fe₂(Et-HPTB)(OBz)](BF₄)₂ (**3a**),¹⁴ were previously reported,¹⁵ and all react with dioxygen at low temperature generating reactive

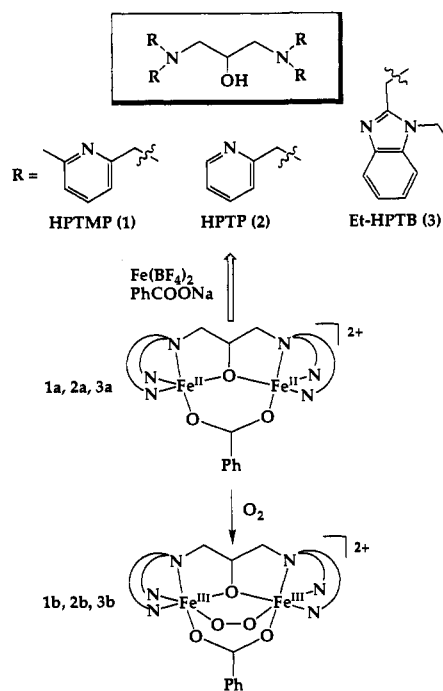


Figure 1. Scheme depicting the ligands, compounds, and reaction investigated here.

diferroc peroxides. Resonance Raman experiments^{12,14,16,17} reveal a symmetric structure consistent with either μ - η^1, η^1 or μ - η^2, η^2 bridging geometry, although the former is preferred.¹⁴ Peroxide complexes **1b–3b** differ in their temperature sensitivity as well as in their ability to oxidize substrates. The reactions of **1a–3a** with dioxygen were investigated by low-temperature stopped-flow spectroscopy.¹⁸ Compounds **2a** and **3a** reacted cleanly with dioxygen and followed a second-order rate law (eqs 1 and 2, Figure S1).^{19–21} A partial order with respect to dioxygen of 0.65



$$\frac{d[B]}{dt} = k_{ox}[2a,3a][O_2] \quad (2)$$

± 0.1 was measured for **1a** (Figure S1). Whereas this value might be rounded to 1, it may also imply a mechanism slightly

(16) Menage, S.; Brennan, B. A.; Juarez-Garcia, C.; Münck, E.; Que, L., Jr. *J. Am. Chem. Soc.* **1990**, *112*, 6423–6425.

(17) Brennan, B. A.; Chen, Q.; Juarez-Garcia, C.; True, A. E.; O'Connor, C. J.; Que, L., Jr. *Inorg. Chem.* **1991**, *30*, 1937–1943.

(18) All kinetics experiments were conducted in dry propionitrile by using a Canterbury low-temperature stopped-flow device (Hi-Tech Scientific). Reactions were initiated by mixing anaerobic ferrous solutions, generally 0.15–0.25 mM, with solvent containing a known dioxygen concentration. Such solutions were generated by saturating solvent with O₂/N₂ gas mixtures. The optical absorbance was monitored at 600 nm. Data were manipulated with the program Kaleidagraph running on a Macintosh IIx computer. At higher temperatures where the peroxide adducts were not stable, isolation techniques were employed, allowing the separation of the formation kinetics from subsequent slower decomposition step(s).

(19) Reaction orders were determined by varying the concentration of one reactant while holding the other conditions constant. For ferrous species, concentrations were varied from 0.02 to 0.75 mM by using serial dilution of a common stock. For dioxygen orders, the ratio of O₂ to N₂ was adjusted with a dynamic gas mixing system (Matheson). This gas mixture was then used to generate a propionitrile solution of known dioxygen concentration (4.4–0.8 mM) at room temperature. The gas concentration at the reduced temperature in the flow lines was adjusted for solvent contraction as described in ref 21.

(20) Quantitative variations in rate constants were sometimes observed among multiply repeated experiments, the maximum error being a factor of 3 in absolute rate. This variation does not affect our conclusions. Its greatest effect is on the activation entropies derived from Eyring plot intercepts.

(21) Karlin, K. D.; Wei, N.; Jung, B.; Kaderli, S.; Niklaus, P.; Zuberbühler, A. D. *J. Am. Chem. Soc.* **1993**, *115*, 9506–9514.

(1) Feig, A. L.; Lippard, S. J. *Chem. Rev.* **1994**, *94*, 759–805.

(2) Que, L., Jr. In *Bioinorganic Catalysis*; Reedijk, J., Ed.; Marcel Dekker: New York, 1993; pp 347–393.

(3) Kurtz, D. M., Jr. *Chem. Rev.* **1990**, *90*, 585–606.

(4) Vincent, J. B.; Olivier-Lilley, G. L.; Averill, B. A. *Chem. Rev.* **1990**, *90*, 1447–1467.

(5) Sanders-Loehr, J. In *Iron Carriers and Iron Proteins*; Loehr, T. M., Ed.; VCH Publishers: New York, 1989; Vol. 5; pp 373–466.

(6) Holmes, M. A.; Le Trong, I.; Turley, S.; Sieker, L. C.; Stenkamp, R. E. *J. Mol. Biol.* **1991**, *218*, 583–593.

(7) Nordlund, P.; Sjöberg, B.-M.; Eklund, H. *Nature* **1990**, *345*, 593–598.

(8) Rosenzweig, A. C.; Frederick, C. A.; Lippard, S. J.; Nordlund, P. *Nature* **1993**, *366*, 537–543.

(9) Bollinger, J. M., Jr.; Edmondson, D. E.; Huynh, B. H.; Filley, J.; Norton, J. R.; Stubbe, J. *Science* **1991**, *253*, 292–298.

(10) Liu, K. E.; Johnson, C. C.; Newcomb, M.; Lippard, S. J. *J. Am. Chem. Soc.* **1993**, *115*, 939–947.

(11) (a) Liu, K. E.; Wang, D.; Huynh, B. H.; Edmondson, D. E.; Salifoglou, A.; Lippard, S. J. *J. Am. Chem. Soc.* **1994**, *116*, 7465. (b) Lee, S.-K.; Fox, B. G.; Froland, W. A.; Lipscomb, J. D.; Münck, E. *J. Am. Chem. Soc.* **1993**, *115*, 6450–6451. (c) Lee, S.-K.; Nesheim, J. C.; Lipscomb, J. D. *J. Biol. Chem.* **1993**, *268*, 21569–21577.

(12) Hayashi, Y.; Suzuki, M.; Uehara, A.; Mizutani, Y.; Kitagawa, T. *Chem. Lett.* **1992**, 91–94.

(13) Although **1** is a known species, the HPTMP ligand was synthesized by a new procedure in which 6-methyl-2-pyridinecarboxaldehyde (Aldrich) was reduced to the alcohol with NaBH₄ in ethanol at 0 °C (91.5% yield). The resultant alcohol was then converted to the bromide by treatment with refluxing 40% H₂SO₄/60% HBr (v/v) for 12 h. The pure bromide was isolated from ether extraction of the neutralized (aqueous Na₂CO₃) reaction mixture (82.5% yield). A 4.6 equiv portion of the bromide was then allowed to react with 1 equiv of 1,3-diamino-2-hydroxypropane (Aldrich) in refluxing aqueous NaOH solution. After purification by silica column chromatography, **1** was isolated in 90.3% yield. The diferrous complex, **1a**, was synthesized in a manner analogous to **2a** and **3a**.

(14) Dong, Y.; Ménage, S.; Brennan, B. A.; Elgren, T. E.; Jang, H. G.; Pearce, L. L.; Que, L., Jr. *J. Am. Chem. Soc.* **1993**, *115*, 1851–1859.

(15) Complexes **1a–3a** were purified by recrystallization from dry MeCN by vapor diffusion of Et₂O under a nitrogen atmosphere.

Table 1. Activation Parameters for the Reaction of Compounds **1a**, **2a**, and **3a** with Dioxygen-Saturated Propionitrile

	ΔH^\ddagger ^a (kJ mol ⁻¹)	ΔS^\ddagger ^a (J mol ⁻¹ K ⁻¹)	ΔH^\ddagger ^b (kJ mol ⁻¹)	ΔS^\ddagger ^b (J mol ⁻¹ K ⁻¹)	$t_{1/2}$ (s ⁻¹) at -60 °C
1a	42.2 ± 1.6	-63 ± 6	39.2 ± 1.6 39.6 ± 2.4	-65 ± 6 -114 ± 9	221 ± 28 ^c
2a	16.5 ± 0.4	-114 ± 2			0.317 ± 0.007
3a	15.4 ± 0.6	-121 ± 3			0.367 ± 0.004
Hr ^d	16.8	-46			

^a Activation parameters in this column are derived from Eyring plots of observed second order rate constants (Figure 2). ^b Activation parameters for **1a** correspond to the composite rate constant $k_{\text{rearr}}k'_{\text{ox}}$ (top value) and k_{rearr} (bottom value) derived from Figure S3. ^c This value is for -45 °C. ^d From *Themiste zostericola* in Tris buffer, pH 8.2, $I = 0.1$ M.²³

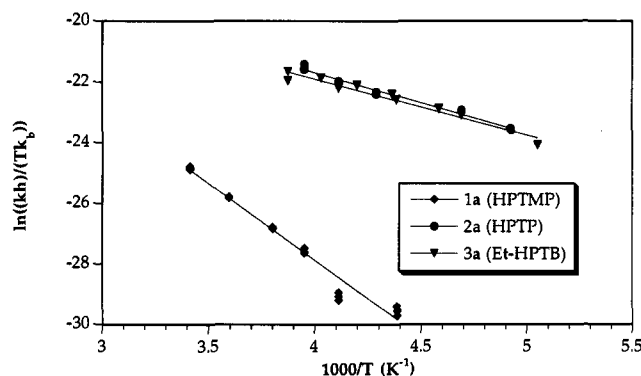
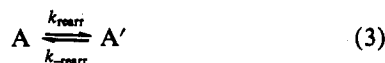


Figure 2. Eyring plot for the reactions of 0.16–0.25 mM **1a**–**3a** with ≈ 4.4 mM dioxygen in propionitrile based on second-order rate constants (Tables S3–S5).

more complex than indicated by eq 1. A reasonable alternative is given in eqs 3 and 4, where an internal rearrangement step is introduced. Steady state analysis yields the modified rate law



in eq 5, which reveals that a partial order between 0 and 1 in dioxygen concentration can be obtained when $k_{\text{rearr}} \sim k'_{\text{ox}}[O_2]$.²²

$$\frac{d[B]}{dt} = \frac{k_{\text{rearr}}k'_{\text{ox}}[1a][O_2]}{k_{\text{rearr}} + k'_{\text{ox}}[O_2]} \quad (5)$$

The rate laws given in eqs 2 and 5 can be differentiated by plotting $1/k_{\text{obs}}$ vs $1/[O_2]$. In the former case, the plot is linear with a zero intercept on the ordinate, whereas a non-zero intercept corresponding to $1/k_{\text{rearr}}$ is obtained for the latter case. When the appropriate double reciprocal plots were made from kinetic data for the reaction of **1a** with varying concentrations of dioxygen, the rate law was clearly seen to be that of eq 5. A similar analysis for the reaction of **2a** with dioxygen revealed the rate law given by eq 2 (Figure S2).

An Eyring analysis of kinetic data collected over the temperature range -75 to 20 °C (Figure 2) afforded the activation parameters listed in Table 1. The ΔH^\ddagger and ΔS^\ddagger values for Hr are provided for comparison.²³ Tables of pseudo-first-order and observed rate constants are available as supplementary material. For the more complicated reaction of **1a**, the activation parameters for k_{rearr} and $k_{\text{rearr}}k'_{\text{ox}}$, derived from Figures S2 and S3, have been separated. Compounds **2a** and **3a** have activation enthalpies quite similar to those of Hr and indicate a simple addition mechanism. The parameters for **1a** differ substantially from

those of the other two compounds. The much larger ΔH^\ddagger value reveals a significant dissociative component to the mechanism. Although strictly speaking the Eyring equation applies only to elementary reactions, the linearity of the plot in Figure 2 reveals that, to a first approximation over the experimental temperature range, the observed rate constant corresponds to a single activation barrier. For **1a**, the observed barrier is dominated by the internal rearrangement step, although the fractional order in dioxygen implies the existence of a temperature regime where the rearrangement and oxidation steps are both partially rate-limiting.

Because the basicity of the nitrogen donor atoms differs only slightly across this series, the different activation parameters for the dioxygen reactivity of **1a** compared with those of **2a** and **3a** are unlikely to have a sizable electronic component. We suggest instead that the significant increase in the activation barrier for **1a** corresponds to a structural rearrangement required to allow inner sphere coordination of O_2 to the metal center. Such a process could arise from substantial elongation or cleavage of an Fe–ligand bond.²⁴ Differences among activation entropies of Hr and the model compounds (Table 1) probably reflect solvent effects and will be discussed in detail elsewhere.

Inner sphere binding of dioxygen to metal centers is required for many metal–dioxygen reactions.²⁵ The mechanistic shift observed in the reaction of **1a**–**3a** with dioxygen underscores its importance in the context of non-heme iron oxidation or hydroxylation systems. Although **1a** has a vacant coordination site for dioxygen binding, it is sterically impeded. In order to react with dioxygen, it must partially or completely dissociate one of its methylpyridyl or carboxylate arms. In the less sterically encumbered complexes, **2a** and **3a**, there is sufficient space to allow access of O_2 without significant reorganization of the coordination sphere and attendant higher activation barrier.

The reaction of dioxygen with the diiron(II) complexes **2a** and **3a** studied here mimics the first step in the chemistry of Hr, namely, coordination of one end of the O_2 molecule to the dimetallic center. In these systems, binding of the second oxygen atom to form the peroxide-bridged diiron(III) unit presumably occurs more rapidly. This chemistry models only the first step of RR and MMO, in which the O–O bond is subsequently cleaved.^{9,11} The fate of the (μ -peroxo)diiron(III) species in both the enzymes and the model compounds and the identification of intermediates along the reaction pathway are currently under investigation.

Acknowledgment. We thank Dr. Andreja Bakac for helpful discussions. This work was supported by grants from the National Institute of General Medical Sciences (GM 32134) and AKZO. A.L.F. acknowledges support from NCI training grant CA09112.

Supplementary Material Available: Figures S1–S3 and Tables S1–S5 presenting kinetic data and derived rate constants (10 pages) for the reactions. This material is contained in many libraries on microfiche, immediately follows this article in the microfilm version of the journal, and can be ordered from the ACS; see any current masthead page for ordering information.

(24) A derivative of **1a** containing a water molecule coordinated to one iron(II) center was shown by X-ray crystallography to have elongated Fe–N bonds, a feature which partially alleviates the stereochemical problem imposed by the pyridyl-6-methyl groups.¹²

(25) Bakac, A.; Espenson, J. H. *Acc. Chem. Res.* **1993**, *26*, 519–523.

(22) This intermediate regime, where both terms contribute, can sometimes be avoided by appropriate choice of experimental conditions. Narrow limits on available conditions imposed by the solubility of O_2 and the temperature instability of the peroxide adducts made such alterations impossible in this case. Moreover, we wished to maintain identical conditions across the series in order to make meaningful comparisons of the kinetic properties of the three compounds.

(23) Petrou, A. L.; Armstrong, F. A.; Sykes, A. G.; Harrington, P. C.; Wilkins, R. G. *Biochim. Biophys. Acta* **1981**, *670*, 377–384.